

## Magnetic and neutron diffraction study on iridium(IV) perovskites $\text{Sr}_2\text{LnIrO}_6$ (Ln = Ce, Tb)

This article has been downloaded from IOPscience. Please scroll down to see the full text article.

2000 J. Phys.: Condens. Matter 12 3229

(<http://iopscience.iop.org/0953-8984/12/14/302>)

View [the table of contents for this issue](#), or go to the [journal homepage](#) for more

Download details:

IP Address: 171.66.16.221

The article was downloaded on 16/05/2010 at 04:45

Please note that [terms and conditions apply](#).

## Magnetic and neutron diffraction study on iridium(IV) perovskites $\text{Sr}_2\text{LnIrO}_6$ (Ln = Ce, Tb)

Daijitsu Harada<sup>†</sup>, Makoto Wakeshima<sup>†</sup>, Yukio Hinatsu<sup>†</sup>, Kenji Ohoyama<sup>‡</sup> and Yasuo Yamaguchi<sup>‡</sup>

<sup>†</sup> Division of Chemistry, Graduate School of Science, Hokkaido University, Sapporo 060-0810, Japan

<sup>‡</sup> Institute for Materials Research, Tohoku University, Sendai 980-8577, Japan

Received 24 August 1999, in final form 23 November 1999

**Abstract.** Powder neutron diffraction measurements have been performed for two tetravalent iridium perovskites,  $\text{Sr}_2\text{CeIrO}_6$  ( $T_N = 21$  K) and  $\text{Sr}_2\text{TbIrO}_6$  ( $T_N = 51$  K). It is found that moments of  $\text{Tb}^{4+}$  in these ordered perovskites are stacked antiferromagnetically along the  $c$ -axis, and the magnetic structure is of type I. The ordered magnetic moment of  $\text{Tb}^{4+}$  is  $4.96 \mu_B$  at 28 K and  $6.60 \mu_B$  at 2 K. From magnetic susceptibility measurements on  $\text{Sr}_2\text{Ce}_x\text{Tb}_{1-x}\text{IrO}_6$ , the antiferromagnetic transition temperatures decrease greatly with decreasing  $\text{Tb}^{4+}$  ion, which indicates that the pathway of such interactions must involve the  $\text{Tb}^{4+}$  ions.

### 1. Introduction

The perovskite-type oxides have the general formula  $\text{ABO}_3$ , in which A represents a large electropositive cation and B represents a small transition metal ion. The perovskite structure can be described as a framework of corner-shared  $\text{BO}_6$  octahedra which contains A cations at 12-coordinate sites. Double perovskite-type oxides have the formula  $\text{A}_2\text{B}'\text{B}''\text{O}_6$ , in which the primes indicate the different ions in different oxidation states, and in some cases, the cations at the B sites,  $\text{B}'$  and  $\text{B}''$ , regularly order, i.e., 1:1 arrangements of  $\text{B}'$  and  $\text{B}''$  ions have been observed over the six-coordinate B sites. Figure 1 illustrates the typical crystal structure of double perovskite,  $\text{Sr}_2\text{LnIrO}_6$ . Since the B cations generally determine the physical properties of perovskites, different kinds of  $\text{B}'$  and  $\text{B}''$  ion should show a variety of the physical properties of double perovskites.

Previously, we reported crystal structures and magnetic properties of iridium perovskites  $\text{Sr}_2\text{LnIrO}_6$  (Ln = Ce, Sm–Lu) [1]. Through their x-ray diffraction measurements, we have found that although the lattice parameters for  $\text{Sr}_2\text{LnIrO}_6$  increase smoothly with the ionic radius of  $\text{Ln}^{3+}$  ion, those for  $\text{Sr}_2\text{CeIrO}_6$  and  $\text{Sr}_2\text{TbIrO}_6$  deviated greatly from this trend. For these experimental results, we have discussed that the Ce and Tb ions are not in the trivalent state, but in the tetravalent state. This consideration has been also supported by the fact that the effective magnetic moment of the terbium ion ( $7.97 \mu_B$ ) obtained from the susceptibility measurements for  $\text{Sr}_2\text{TbIrO}_6$  accords with the theoretical moment for the  $\text{Tb}^{4+}$  ion ( $7.94 \mu_B$ ) (for the  $\text{Tb}^{3+}$  ion, the moment is calculated to be  $9.72 \mu_B$ ). The results of the magnetic susceptibility measurements are that these  $\text{Sr}_2\text{LnIrO}_6$  compounds are paramagnetic and that among them,  $\text{Sr}_2\text{CeIrO}_6$  and  $\text{Sr}_2\text{TbIrO}_6$  show the antiferromagnetic transition at 21 and 51 K,

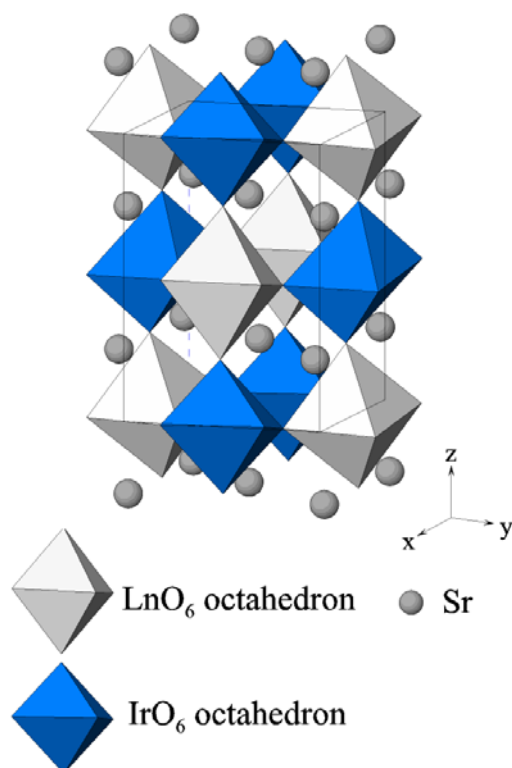


**Figure 1.** The crystal structure of  $\text{Sr}_2\text{LnIrO}_6$ .

respectively. Figures 2 and 3 show the temperature dependence of magnetic susceptibilities for these compounds. In addition to the magnetic transition at 51 K,  $\text{Sr}_2\text{TbIrO}_6$  shows another anomaly at 27 K in its magnetic susceptibility–temperature curve (see figure 3). As far as we know, there was no report on the magnetic properties of compounds in which iridium and lanthanide elements are contained. Very recently, we have published magnetic properties of  $\text{A}_2\text{RIrO}_6$  ( $\text{A} = \text{Sr}, \text{Ba}$ ;  $\text{R} = \text{Sc}, \text{Y}, \text{La}, \text{Lu}$ ) [2] in which only  $\text{Ir}^{5+}$  are magnetic ions. They are all paramagnetic down to 2 K, i.e. no magnetic cooperative phenomena have been found in these compounds.

In this paper, we focus our attention on the magnetic properties of  $\text{Sr}_2\text{CeIrO}_6$  and  $\text{Sr}_2\text{TbIrO}_6$ . In the  $\text{Sr}_2\text{TbIrO}_6$ , there are two kinds of magnetic ion, i.e.  $\text{Tb}^{4+}$  and  $\text{Ir}^{4+}$  ions. The electronic structures of these ions are  $[\text{Xe}]4f^7$  and  $[\text{Xe}]4f^{14}5d^5$ , respectively, where  $[\text{Xe}]$  is the xenon core. Therefore, we can expect to observe magnetic cooperative phenomena caused by these 4f and 5d electrons. Battle *et al* reported magnetic properties of double-perovskite-type oxides such as  $\text{Ca}_2\text{LaRuO}_6$ ,  $\text{Sr}_2\text{YRuO}_6$ ,  $\text{Ca}_2\text{HoRuO}_6$ ,  $\text{Ca}_2\text{YRuO}_6$  [3–6], and determined their magnetic structures to be type I antiferromagnetic.

We have performed powder neutron diffraction measurements for both the compounds to elucidate their magnetic structures in the antiferromagnetic state. In addition, magnetic susceptibilities of solid solutions  $\text{Sr}_2\text{Ce}_x\text{Tb}_{1-x}\text{IrO}_6$  have been measured to clarify the anomaly found in the susceptibility of  $\text{Sr}_2\text{TbIrO}_6$  and to obtain information on the magnetic interaction between 5d and 4f electrons.

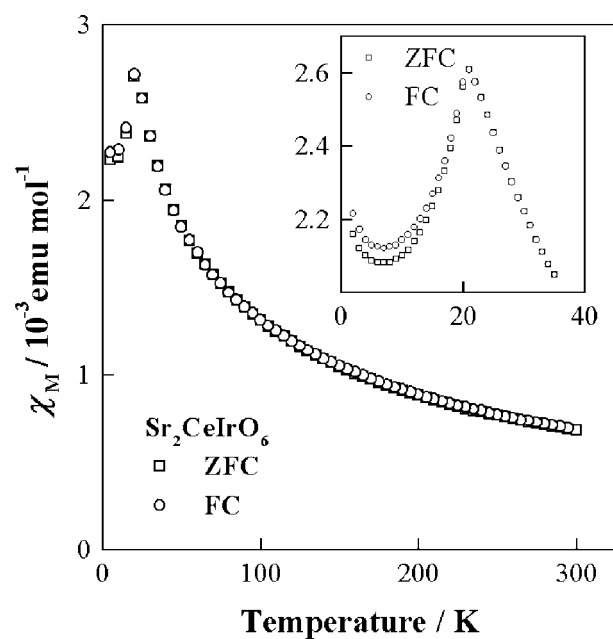


Figure 2. Temperature dependence of the magnetic susceptibilities of  $\text{Sr}_2\text{CeIrO}_6$ .

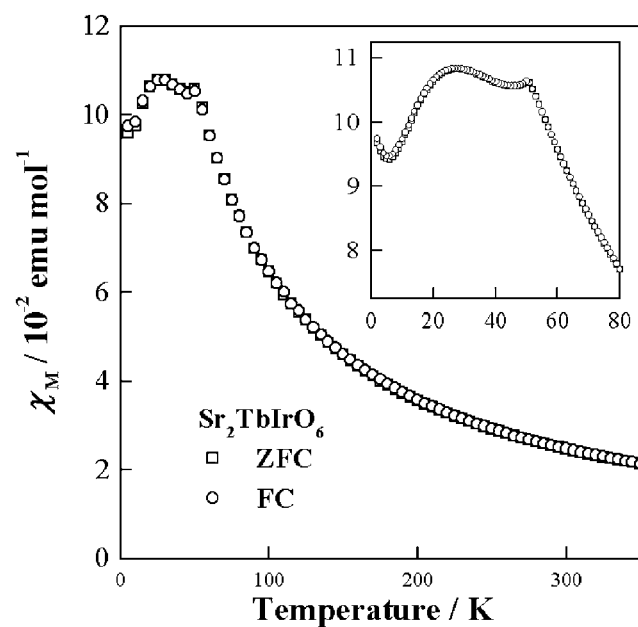


Figure 3. Temperature dependence of the magnetic susceptibilities of  $\text{Sr}_2\text{TbIrO}_6$ .

## 2. Experiment

Sintered materials of  $\text{Sr}_2\text{Ce}_x\text{Tb}_{1-x}\text{IrO}_6$  ( $x = 0, 0.1, 0.2, \dots, 1.0$ ) were prepared. Powders of  $\text{SrCO}_3$ ,  $\text{CeO}_2$ ,  $\text{Tb}_4\text{O}_7$  and Ir were weighed in the appropriate metal ratios, and were ground

intimately in an agate mortar. The mixtures were pressed into pellets and then calcined in air at 900 °C for 12 h. The samples were heated again in air at 1200 °C for 72–96 h with several interval grindings.

Powder x-ray diffraction profiles for these solid solutions were recorded, with Cu K $\alpha$  radiation on a Rigaku RINT 2000 diffractometer equipped with a curved graphite monochromator in the range  $10^\circ \leq \theta \leq 120^\circ$  at intervals of  $0.02^\circ$ . The structures were refined with the Rietveld analysis method, using the Rietan program [8].

Powder neutron diffraction profiles for Sr<sub>2</sub>CeIrO<sub>6</sub> and Sr<sub>2</sub>TbIrO<sub>6</sub> were measured in the range  $3^\circ \leq \theta \leq 153^\circ$  at intervals of  $0.1^\circ$  at wavelength of 1.819 Å. Measurements were performed by the Kinken powder diffractometer for high efficiency and high resolution measurements, HERMES, of the institute for Materials Research, Tohoku University [9], installed at the JRR-3M reactor in Japan Atomic Energy Research Institute Tokai, Japan. Since Sr<sub>2</sub>CeIrO<sub>6</sub> shows an antiferromagnetic transition temperature at  $T_N = 21$  K, measurements were made both at 2 K ( $T < T_N$ ) and at 30 K ( $T > T_N$ ). For Sr<sub>2</sub>TbIrO<sub>6</sub> showing both the antiferromagnetic transition at  $T_N = 51$  K and a certain anomaly at about  $T_A = 27$  K, measurements were made at 2 K ( $T < T_A < T_N$ ), 28 K ( $T_A < T < T_N$ ) and 60 K ( $T_A < T_N < T$ ).

The temperature dependence of magnetic susceptibilities for Sr<sub>2</sub>Ce<sub>x</sub>Tb<sub>1-x</sub>IrO<sub>6</sub> ( $x = 0, 0.1, 0.2, \dots, 1.0$ ) was measured with a SQUID (Quantum Design, MPMS model) under the zero-field-cooled condition (ZFC). It was measured on heating the samples to 80 K after zero-field cooling to 2 K. The applied magnetic field was 0.1 T. Magnetic susceptibility for these compounds does not depend on the applied magnetic field up to 5.0 T. The temperature dependence of the susceptibility under the field-cooled condition (FC) was not measured, because we have previously found that there was no divergence between the ZFC and the FC magnetic susceptibilities for these compounds [1].

### 3. Results and discussion

#### 3.1. Neutron diffraction measurements

**3.1.1. Sr<sub>2</sub>CeIrO<sub>6</sub>.** Our previous x-ray diffraction measurements on Sr<sub>2</sub>CeIrO<sub>6</sub> and Sr<sub>2</sub>TbIrO<sub>6</sub> show that these two compounds both have the monoclinic perovskite structure with the space group  $P2_1/n$ . Figure 4 shows the neutron diffraction profiles for Sr<sub>2</sub>CeIrO<sub>6</sub> measured at 2 and 30 K. The results of the crystal structure determination on Sr<sub>2</sub>CeIrO<sub>6</sub> by the present neutron diffraction measurements are given in table 1 together with those by the x-ray diffraction measurements. The results of neutron diffraction measurements performed at 2 and 30 K agree well with the x-ray diffraction results, which means that the crystal phase transition does not occur at low temperatures. Atomic positions of strontium occupying the A site of the perovskite structure are well in accordance between x-ray diffraction measurement and neutron diffraction measurement. But the atomic positions of oxygen are a little in disagreement between these measurements. We consider that the results by neutron diffraction measurements are more reliable, because x-ray diffraction measurements have a disadvantage for determining the positions of light atoms. With decreasing temperature (from room temperature to 30 K), lattice parameters of Sr<sub>2</sub>CeIrO<sub>6</sub> decrease.

Since Sr<sub>2</sub>CeIrO<sub>6</sub> shows the antiferromagnetic transition at 21 K, magnetic Bragg peaks should appear in the neutron diffraction profile measured at 2 K. However, no difference in the neutron diffraction profiles measured at 2 K and at 30 K was observed (figure 4). Currie *et al* [7] reported that magnetic Bragg peaks were not observed in the neutron diffraction measurements of a double perovskite La<sub>2</sub>CoIrO<sub>6</sub> which is isostructural with our samples

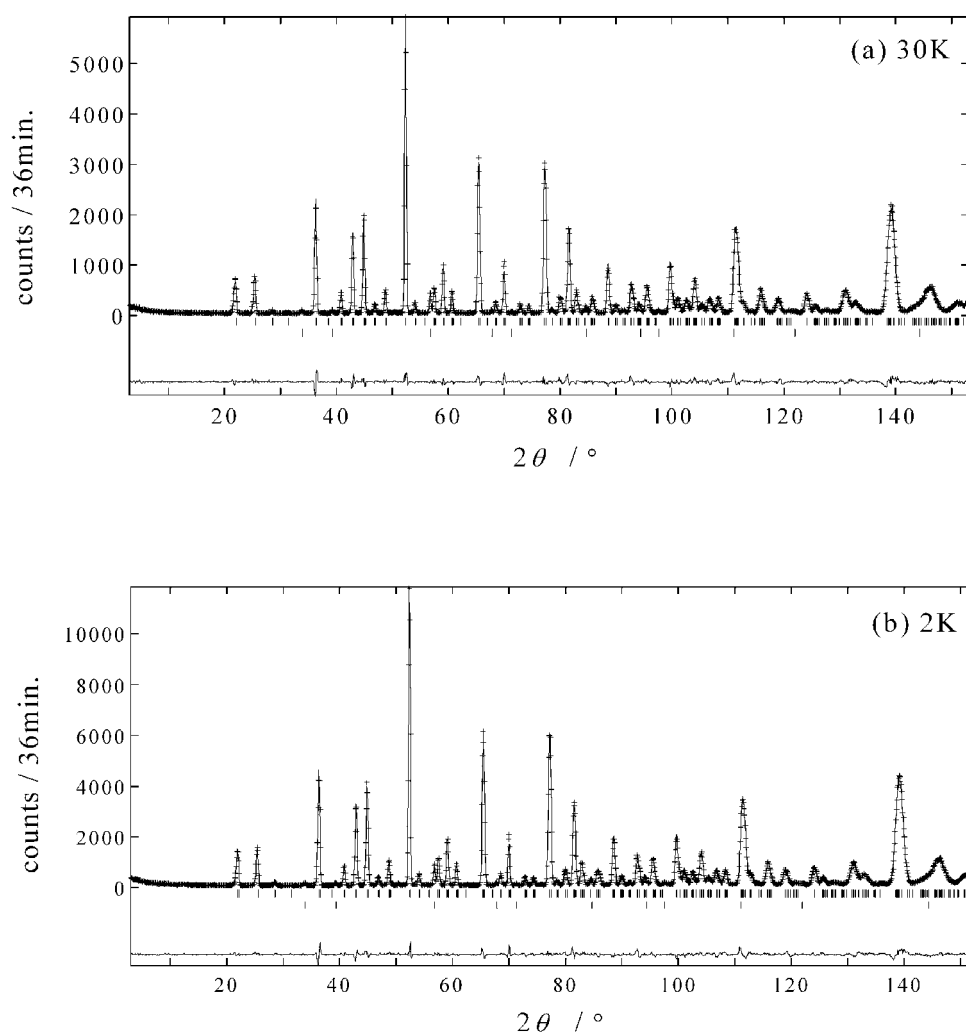


**Figure 4.** Neutron diffraction profiles for  $\text{Sr}_2\text{CeIrO}_6$  at (a) 30 K and (b) 2 K.

$\text{Sr}_2\text{LnIrO}_6$  ( $\text{Ln} = \text{Ce}, \text{Tb}$ ). We consider that since the magnetic moment of the  $\text{Ir}^{4+}$  ion which is the only magnetic ion in  $\text{Sr}_2\text{CeIrO}_6$  is very small, magnetic diffraction peaks are not detected.

**3.1.2.  $\text{Sr}_2\text{TbIrO}_6$ .** The magnetic susceptibility measurement on  $\text{Sr}_2\text{TbIrO}_6$  shows the antiferromagnetic transition at 51 K ( $T_N$ ) and another anomaly at about 27 K ( $T_A$ ). Therefore, we performed our neutron diffraction measurements at three temperatures, 60 K ( $T_N < T$ ), 28 K ( $T_A < T < T_N$ ) and 2 K ( $T < T_A$ ). Figure 5 shows the observed and calculated neutron diffraction profiles. The atomic parameters for  $\text{Sr}_2\text{TbIrO}_6$  after the refinement of the neutron diffraction profiles are given in table 2 together with those by the x-ray diffraction measurements. All the diffraction peaks measured at 60 K can be indexed in a monoclinic unit cell with space group  $P2_1/n$ . In the profiles measured at 28 and at 2 K, magnetic Bragg reflections in addition to the nuclear Bragg reflections appear. These magnetic Bragg peaks are due to the alignment of the  $\text{Tb}^{4+}$  moment. Magnetic Bragg reflections due to the alignment of

**Table 1.** Crystal and magnetic structure data for Sr<sub>2</sub>CeIrO<sub>6</sub>.

Atoms	Position	<i>x</i>	<i>y</i>	<i>z</i>
X-ray diffraction at RT				
<i>a</i> = 5.8341(3) Å <i>b</i> = 5.8436(3) Å <i>c</i> = 8.2559(6) Å $\beta$ = 90.195(4)° <i>V</i> = 281.46(3) Å <sup>3</sup>				
<i>R</i> <sub>wp</sub> = 12.09% <i>R</i> <sub>I</sub> = 2.48% <i>R</i> <sub>F</sub> = 2.35%				
Sr	4e	0.497(2)	0.530(1)	0.255(2)
Ce	2d	0.5	0.0	0.0
Ir	2c	0.5	0.0	0.5
O1	4e	0.26(1)	0.29(1)	0.04(1)
O2	4e	0.19(1)	0.77(1)	0.02(1)
O3	4e	0.59(1)	−0.01(1)	0.26(1)
Neutron diffraction at 30 K				
<i>a</i> = 5.8165(3) Å <i>b</i> = 5.8389(3) Å <i>c</i> = 8.2337(5) Å $\beta$ = 90.227(4)° <i>V</i> = 279.64(3) Å <sup>3</sup>				
<i>Q</i> = 1.71(5) <i>R</i> <sub>wp</sub> = 9.07% <i>R</i> <sub>I</sub> = 1.50% <i>R</i> <sub>F</sub> = 0.75%				
Sr	4e	0.492(1)	0.532(1)	0.252(2)
Ce	2d	0.5	0.0	0.0
Ir	2c	0.5	0.0	0.5
O1	4e	0.273(1)	0.296(2)	0.038(1)
O2	4e	0.198(2)	0.774(2)	0.040(1)
O3	4e	0.573(2)	−0.016(1)	0.263(1)
Neutron diffraction at 2 K				
<i>a</i> = 5.8180(3) Å <i>b</i> = 5.8402(2) Å <i>c</i> = 8.2355(4) Å $\beta$ = 90.225(3)° <i>V</i> = 279.82(2) Å <sup>3</sup>				
<i>Q</i> = 1.83(5) <i>R</i> <sub>wp</sub> = 9.25% <i>R</i> <sub>I</sub> = 1.41% <i>R</i> <sub>F</sub> = 0.71%				
Sr	4e	0.492(1)	0.532(1)	0.252(1)
Ce	2d	0.5	0.0	0.0
Ir	2c	0.5	0.0	0.5
O1	4e	0.273(1)	0.296(2)	0.038(1)
O2	4e	0.197(1)	0.775(2)	0.041(1)
O3	4e	0.572(2)	−0.016(1)	0.263(1)

Definitions of reliability factors *R*<sub>WP</sub>, *R*<sub>I</sub> and *R*<sub>F</sub> are given as follows,

$$R_{WP} = [\sum w(|F(o)| - |F(c)|)^2 / \sum w|F(o)|^2]^{1/2}, R_I = \sum |I_k(o) - I_k(c)| / \sum I_k(o)$$

and  $R_F = \sum [|I_k(o)|^{1/2} - |I_k(c)|^{1/2}] / \sum |I_k(o)|^{1/2}$ .

the magnetic moments of Ir<sup>4+</sup> ions do not appear experimentally, which is in accordance with the result for Sr<sub>2</sub>CeIrO<sub>6</sub>. The large (100) and (010) peaks ( $2\theta \cong 18.2^\circ$ ) are observed in the profiles measured at 28 and at 2 K, but the intensity of the (001) diffraction ( $2\theta \cong 12.8^\circ$ ) is very weak. This fact indicates that the magnetic moments of Sr<sub>2</sub>TbIrO<sub>6</sub> are aligned almost along the *c*-axis. We expect that the magnetic structure is of the antiferromagnetic type I (figure 6) from the magnetic Bragg peaks. The Rietveld analysis assuming the type I magnetic structure gives the most reliable results.

A Tb<sup>4+</sup> ion has 12 nearest neighbour Tb<sup>4+</sup> ions (NN) and six next-nearest neighbours (NNN). The type I magnetic structure consists of eight nearest neighbours antiferromagnetically coupled to the central ion, four nearest neighbours in the *c* planar ferromagnetically coupled and all six next-nearest neighbours ferromagnetically coupled. Battle *et al* [3–6] discussed the dominant magnetic interactions in such a structure, which was either those between NN or those between NNN for Ca<sub>2</sub>LaRuO<sub>6</sub>, Ba<sub>2</sub>LaRuO<sub>6</sub>, Ca<sub>2</sub>LaRuO<sub>6</sub>, Sr<sub>2</sub>YRuO<sub>6</sub>. Since two kinds of magnetic ion, Ir and Tb, are involved in the case of Sr<sub>2</sub>TbIrO<sub>6</sub>, the interaction between Ir and Tb should be considered, which means that the dominant pathway of magnetic interactions is very complicated.

The ordered magnetic moments at 28 and at 2 K are calculated to be 4.94 and 6.60 μ<sub>B</sub>, respectively. The saturated magnetic moment for the Tb<sup>4+</sup> ion (4f<sup>7</sup>) is 7.0 μ<sub>B</sub>. Although the

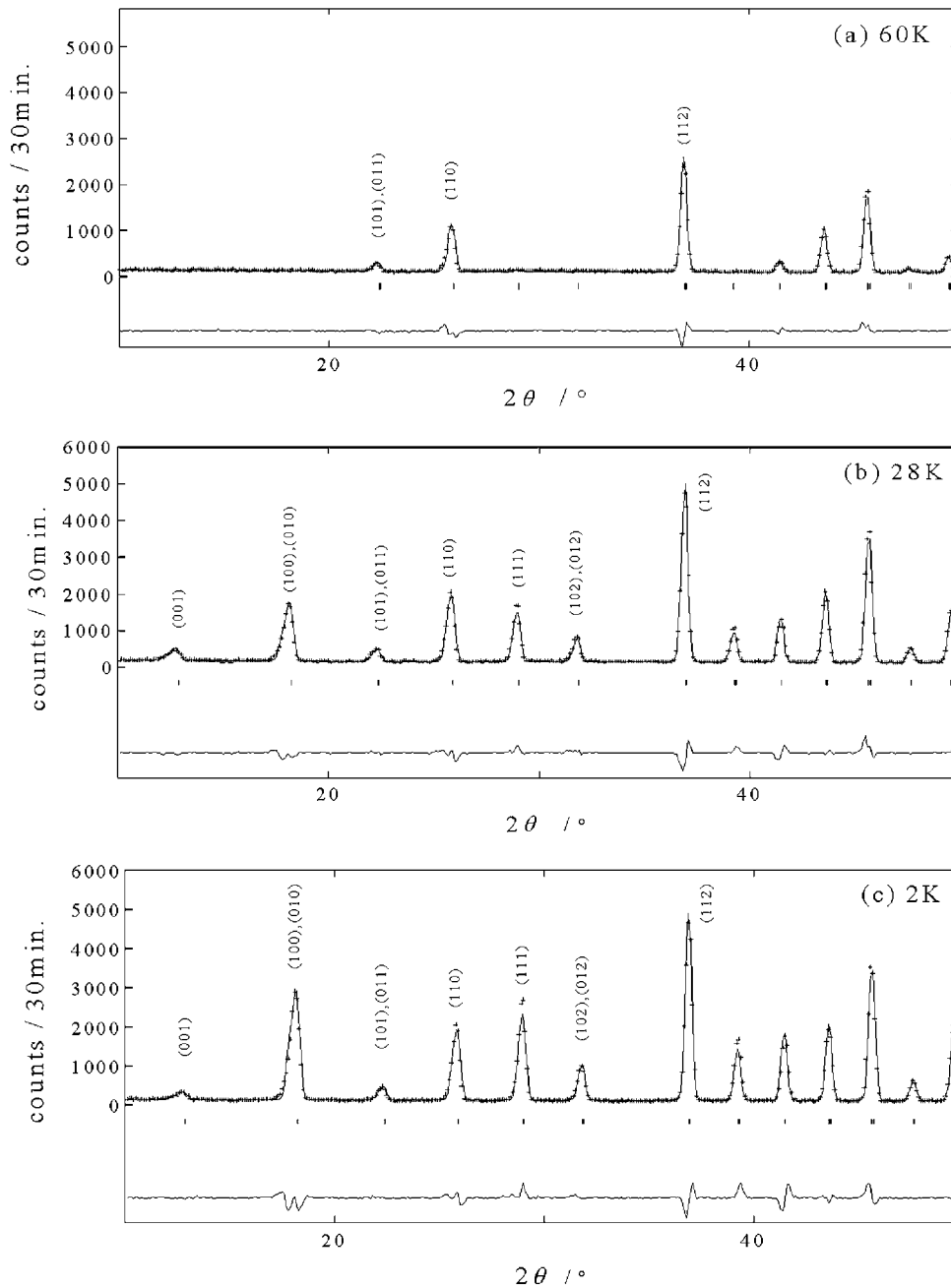


Figure 5. Neutron diffraction profiles for  $\text{Sr}_2\text{TbIrO}_6$  at (a) 60 K, (b) 28 K and (c) 2 K.

moment at 2 K is larger than that at 28 K, the intensity of the (001) reflection at 2 K is weaker than that at 28 K (see figure 7). This result indicates that the angle between the direction of the moment and the  $c$ -axis at 2 K is smaller than that at 28 K, and that the magnetic moment of the  $\text{Tb}^{4+}$  ion orders remarkably with decreasing temperature. Although the anomaly has been found at 27 K in the susceptibility–temperature curve, there is no difference in the diffraction



**Table 2.** Crystal and magnetic structure data for Sr<sub>2</sub>TbIrO<sub>6</sub>.

Atoms	Position	<i>x</i>	<i>y</i>	<i>z</i>
X-ray diffraction at RT				
$a = 5.7604(2) \text{ \AA}$ $b = 5.7506(2) \text{ \AA}$ $c = 8.1371(3) \text{ \AA}$ $\beta = 90.089(2)^\circ$ $V = 269.55(1) \text{ \AA}^3$				
$R_{wp} = 9.72\%$ $R_I = 1.75\%$ $R_F = 2.10\%$				
Sr	4e	0.492(1)	0.521(1)	0.247(1)
Tb	2d	0.5	0.0	0.0
Ir	2c	0.5	0.0	0.5
O1	4e	0.28(1)	0.29(1)	0.04(1)
O2	4e	0.22(1)	0.76(1)	0.02(1)
O3	4e	0.56(1)	-0.01(1)	0.26(1)
Neutron diffraction at 60 K				
$a = 5.7431(4) \text{ \AA}$ $b = 5.7440(4) \text{ \AA}$ $c = 8.1147(5) \text{ \AA}$ $\beta = 90.148(5)^\circ$ $V = 267.69(3) \text{ \AA}^3$				
$Q = 0.61(6)$ $R_{wp} = 10.30\%$ $R_I = 2.66\%$ $R_F = 1.39\%$				
Sr	4e	0.495(2)	0.525(1)	0.250(2)
Tb	2d	0.5	0.0	0.0
Ir	2c	0.5	0.0	0.5
O1	4e	0.272(2)	0.284(3)	0.036(2)
O2	4e	0.209(2)	0.780(3)	0.032(2)
O3	4e	0.560(2)	-0.012(2)	0.259(2)
Neutron diffraction at 28 K				
$a = 5.7464(4) \text{ \AA}$ $b = 5.7463(3) \text{ \AA}$ $c = 8.1234(5) \text{ \AA}$ $\beta = 90.134(5)^\circ$ $V = 267.79(3) \text{ \AA}^3$				
$Q = 0.79(4)$ $R_{wp} = 8.98\%$ $R_I = 3.22\%$ $R_F = 1.96\%$				
Sr	4e	0.494(2)	0.529(1)	0.246(1)
Tb	2d	0.5	0.0	0.0
Ir	2c	0.5	0.0	0.5
O1	4e	0.273(2)	0.288(2)	0.032(1)
O2	4e	0.212(2)	0.780(2)	0.029(1)
O3	4e	0.566(2)	-0.013(2)	0.259(1)
Magnetic moment: $4.96 \mu_B$				
Angle between the moment and the <i>c</i> -axis: $28.67^\circ$				
Neutron diffraction at 2 K				
$a = 5.7464(4) \text{ \AA}$ $b = 5.7461(3) \text{ \AA}$ $c = 8.1243(4) \text{ \AA}$ $\beta = 90.143(5)^\circ$ $V = 267.95(3) \text{ \AA}^3$				
$Q = 1.03(5)$ $R_{wp} = 9.92\%$ $R_I = 3.21\%$ $R_F = 1.66\%$				
Sr	4e	0.494(2)	0.530(1)	0.247(2)
Tb	2d	0.5	0.0	0.0
Ir	2c	0.5	0.0	0.5
O1	4e	0.273(2)	0.289(2)	0.031(1)
O2	4e	0.213(2)	0.779(2)	0.029(1)
O3	4e	0.566(2)	-0.015(1)	0.259(1)
Magnetic moment: $6.60 \mu_B$				
Angle between the moment and the <i>c</i> -axis: $16.96^\circ$				

profiles between that at 2 K and at 28 K, i.e. no new magnetic Bragg peaks appear between them.

To obtain information on the anomaly in the magnetic susceptibility, we have measured the temperature dependence of the diffraction peaks for Sr<sub>2</sub>TbIrO<sub>6</sub> in the temperature range of 2 K to 60 K at intervals of 2–3 K. Unfortunately, no remarkable change was found in the neutron diffraction profiles. We believe that since the anomaly is found as a broad maximum in the susceptibility–temperature curve, the corresponding magnetic Bragg peaks are very weak and therefore they are hidden in the errors of the neutron diffraction experiment.

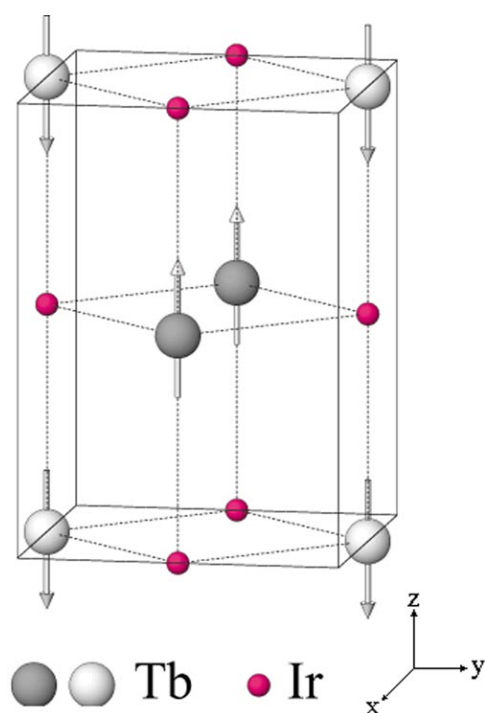


**Figure 6.** The type I magnetic structure of  $\text{Sr}_2\text{TbIrO}_6$ . Only terbium and iridium ions are depicted.

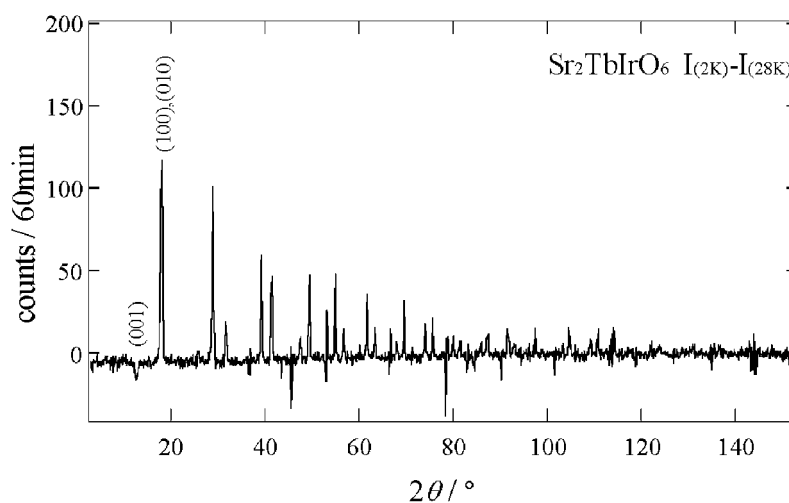


**Figure 7.** The difference in the intensity of neutron diffraction profiles for  $\text{Sr}_2\text{TbIrO}_6$  between that at 2 K and at 28 K.

### 3.2. Magnetic susceptibility measurement for solid solutions $\text{Sr}_2\text{Ce}_x\text{Tb}_{1-x}\text{O}_6$

The temperature dependence of the magnetic susceptibilities for  $\text{Sr}_2\text{Ce}_x\text{Tb}_{1-x}\text{IrO}_6$  ( $x = 0.0, 0.2, 0.4, 0.6, 0.7, \dots, 1.0$ ) was measured under the zero-field-cooled condition (ZFC), and the results are shown in figure 8. Since the magnetic moment of the  $\text{Ir}^{4+}$  ion is rather smaller than

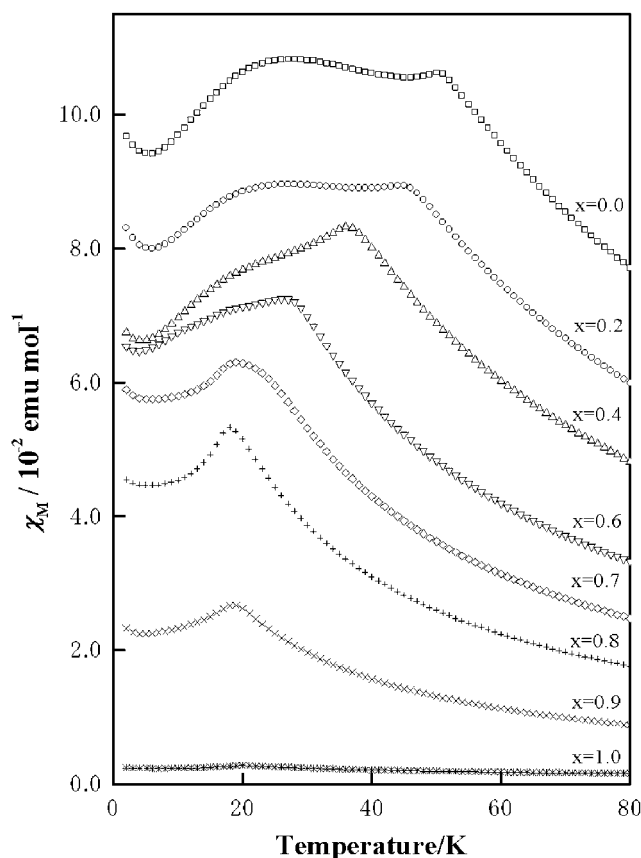


**Figure 8.** Temperature dependence of the magnetic susceptibilities of  $\text{Sr}_2\text{Ce}_x\text{Tb}_{1-x}\text{IrO}_6$  ( $x = 0.0, 0.2, 0.4, 0.6, 0.7, 0.8, 0.9, 1.0$ ).

that of the  $\text{Tb}^{4+}$  ion, the magnetic susceptibilities of  $\text{Sr}_2\text{Ce}_x\text{Tb}_{1-x}\text{IrO}_6$  ( $0.0 \leq x \leq 0.9$ ) are almost entirely due to the  $\text{Tb}^{4+}$  ion. As the  $x$  value increases (the ratio of  $\text{Tb}^{4+}$  decreases), the antiferromagnetic transition temperature  $T_N = 51$  K (for  $\text{Sr}_2\text{TbIrO}_6$ ,  $x = 0.0$ ) decreases and the maximum in the susceptibility–temperature curve becomes broad. The anomaly found at  $T_A = 27$  K becomes ambiguous and its temperature decreases with increasing  $x$  value. For the compounds with  $x \geq 0.8$  the anomaly peaks in the susceptibility against temperature disappear.

Now, we will discuss the pathway of the antiferromagnetic interaction found in  $\text{Sr}_2\text{Ce}_x\text{Tb}_{1-x}\text{IrO}_6$ . In this case, three kinds of interaction are predicted, (i) the interactions between  $\text{Tb}^{4+}$  ions along the pathway of nearest neighbours (NN) or next-nearest neighbours (NNN), (ii) the interactions between  $\text{Tb}^{4+}$  and  $\text{Ir}^{4+}$  along the pathway of  $\text{Tb-O-Ir}$  and (iii) the interactions between  $\text{Ir}^{4+}$  ions along the pathway of nearest neighbours or next-nearest neighbours. Experimental results that the antiferromagnetic transition temperature ( $T_N$ ) for  $\text{Sr}_2\text{Ce}_x\text{Tb}_{1-x}\text{IrO}_6$  decreases greatly with decreasing ratio of  $\text{Tb}^{4+}$ , and the temperature of the anomaly in the magnetic susceptibility at  $T_A = 27$  K is relatively insensitive to decreasing of the ratio of  $\text{Tb}^{4+}$  ions indicate that the pathway of magnetic interactions at  $T_N = 51$  K must involve  $\text{Tb}^{4+}$  ions, i.e. (i) or (ii).

**References**

- [1] Harada D, Wakeshima M and Hinatsu Y 1999 *J. Solid State Chem.* **145** 256
- [2] Wakeshima M, Harada D and Hinatsu Y 1999 *J. Alloys Compounds* **287** 130
- [3] Battle P D, Goodenough J B and Price R 1983 *J. Solid State Chem.* **46** 234
- [4] Battle P D and Macklin W J 1984 *J. Solid State Chem.* **54** 245
- [5] Battle P D and Macklin W J 1984 *J. Solid State Chem.* **52** 138
- [6] Battle P D and Jones C W 1991 *J. Solid State Chem.* **90** 302
- [7] Currie R C, Vente J F, Frikkee E and Ijdo D J W 1995 *J. Solid State Chem.* **116** 199
- [8] Izumi F 1993 *The Rietveld Method* ed R A Young (Oxford: Oxford University Press) ch 13
- [9] Ohoyama K, Kanouchi T, Nemoto K, Oheshi M, Kajitani T and Yamaguchi Y 1998 *Japan. J. Appl. Phys.* **37** 3319